JOURNAL OF MATERIALS SCIENCE: MATERIALS IN ELECTRONICS 9 (1998) 145–150

Effect of MgO addition on the electrical transport properties of highly Sb-doped $BaTiO_3$ ceramics

BI-SHIOU CHIOU, I-HORN WANG
Dept. of Electronics Engineering and Institute of Electronics, National Chiao Tung University, Hsinchu, Taiwan

$BaTiO_3$ ceramics doped with Sb donors and Mg acceptors have been fabricated. The lattice constant ratio c/a and the Curie point T_c decrease with increasing Sb concentration. The minimum room temperature resistivity ρ_{min} of the codoped $BaTiO_3$ occurs at a composition of 0.9 mole% Sb_2O_3-1 mole % MgO as compared to the literature reported ρ_{min} at 0.3 mole % antimony for the Sb_2O_3-doped $BaTiO_3$. The Mg^{2+} ion acts as an acceptor in the $BaTiO_3$ ceramics, which compensates the donor contribution from Sb^{3+} and shifts the doped-$BaTiO_3$ semiconducting region to higher antimony content. The calculated donor concentration confirms the compensation effect of Mg acceptors over Sb donors. The temperature dependence of both barrier height and dielectric constant of specimens is discussed.

1. Introduction

Barium titanate has attracted much attention in the field of electronic ceramics. Doped, n-type barium titanate ceramics exhibit an abrupt rise in resistivity near the Curie temperature (T_c): the so-called positive temperature coefficient of resistivity (PTCR) effect. This anomaly of resistivity renders barium titanate useful in various applications [1, 2]. Many factors affect the PTCR phenomena of $BaTiO_3$ ceramics such as: the concentration and the distribution of the trace additives [2–6], the impurities in the raw materials, and the firing conditions [7–9].

The U-shaped relation between the dopant ion content and the resistivity of semiconducting $BaTiO_3$ is well known [5]. For Sb_2O_3-doped $BaTiO_3$, the minimum resistivity exists at 0.3 mole % content of antimony dopant. However, an insulating $BaTiO_3$ is obtained beyond that range [10]. Previous work by Chiou *et al.* [7] reported that the Curie point of $BaTiO_3$-based ceramics was altered by addition of Sb_2O_3 and the dielectric peak was maintained by the presence of MgO additive. In addition, the presence of magnesium ions, which acted as acceptors, pushed the $BaTiO_3$ semiconducting region to higher Sb_2O_3 content. However, the effect of MgO on Sb-doped $BaTiO_3$ is not well known.

In this study, the dielectric properties and PTCR effect of MgO-Sb_2O_3 codoped $BaTiO_3$ are investigated. The antimony dopant content employed is larger than normally reported [11]. The doping concentrations in these specimens are 1 mole % MgO, 0.05 mole % MnO_2, and 0.8 to 1.0 mole % Sb_2O_3. The addition of MnO_2 enhances the PTCR effect [7]. Manganese is an acceptor dopant. Ting *et al.* [12] reported that the acceptor effect of Mn^{2+} became pronounced only at an Mn^{2+} concentration of above 0.05 mole %. Illingsworth *et al.* [17] found that a small addition of Mn (0.04 mole %) to $BaTiO_3$ had negligible effect on both the bulk resistance and the dielectric constant above T_c. A 0.05 mole % MnO_2 addition in this study optimizes the PTCR phenomena while minimizing the acceptor effect of Mn^{2+}. The possible role of Mg in the PTCR behaviour of highly Sb-doped $BaTiO_3$ is discussed.

2. Experimental procedures

Samples were prepared by a conventional ceramic fabrication process. Appropriate amounts of $BaCO_3$, TiO_2, MgO, MnO_2, and Sb_2O_3 (reagent grade, Merck & Co. Inc., Darmstadt, Germany), together with ethyl alcohol, were ball-milled for 24 h. The molar ratio of $BaCO_3$ and TiO_2 was 1:1.01, excess TiO_2 was added to obtain a TiO_2-rich liquid phase during sintering [7]. After drying, the mixture was calcined in an alumina crucible at 1100 °C for 2 h, then crushed into powder and pressed into a disk-shape specimen, 10 mm in diameter and 1.5 mm in thickness. Sintering was carried out with an initial heating rate of 100 °C min^{-1} to 1200 °C, and held at 1200 °C for 6 min, then heated to 1400 °C at 100 °C min^{-1} and held at 1400 °C for 18 min. The two-stage firing resulted in a more uniform microstructure than a single-stage firing [7]. After sintering, electrodes were applied to the specimens by rubbing In-Ga (40:60) alloy on both surfaces to provide ohmic contacts.

The resistance of samples was measured with a pA meter (HP4140B, Hewlett Packard). The impedence of samples was measured with an impedence analyser (HP4192A). The densities of the sintered specimens were determined by the Archimedes method. Microstructure and elemental distribution of the samples

were examined with a scanning electron microscope (SEM, Hitachi, S-570) and an electron microprobe analyser (EPMA, JEOL JCXA-733, Japan). Phase identification of the samples was carried out with an X-ray diffractometer. The average grain size of the sample was determined by the linear intercept method from the scanning electron micrograph of the as-fired surface.

3. Results and discussion

The microstructures for Sb_2O_3-doped $BaTiO_3$ are shown in Fig. 1. The average grain size is 9.2, 7.0, and 5.0 μm for samples doped with 0.8, 0.9, and 1.0 mole % Sb_2O_3, respectively. Addition of Sb_2O_3 inhibits the grain growth of $BaTiO_3$ ceramics. The X-ray diffraction (XRD) patterns indicate that the specimens are of perovskite structure. The lattice constant as a function of Sb_2O_3 concentration is calculated on the basis of the XRD results and shown in Fig. 2. In contrast to the decrease in lattice constant c, lattice constant a increases and the c/a ratio decreases with increasing Sb content. At room temperature a and c for pure $BaTiO_3$ are 0.3992 nm and 0.4035 nm, respectively. These values are not obtained by extrapolating data in Fig. 2 at 0 mole % Sb_2O_3, because two other additives, MgO and MnO_2, are present in $BaTiO_3$ ceramics. The theoretical density D_{th} is calculated from the lattice constants. Table I lists the grain size and the measured and theoretical density of the specimens. The percentage of the D_{th} increases with Sb_2O_3 content, the 97.5% D_{th} is obtained for the 1.0 mole % Sb_2O_3 sample. Figs 3 and 4 show the temperature variation of the dielectric constant and dissipation factor of the Sb_2O_3-doped $BaTiO_3$, respectively. The Curie temperatures are 64 °C, 60 °C, and 55 °C for the 0.85, 0.9, and 1.0 mole % specimens, respectively.

The resistivity ρ as a function of temperature is given in Fig. 5. The resistivity decreases initially and then increases as the Sb_2O_3 content increases from 0.85 mole % to 1.0 mole %. The specimen with 0.9 mole % Sb_2O_3 has the lowest resistivity. The room temperature resistivity for the 0.9 mole % Sb_2O_3-MgO codoped sample is $\sim 240\ \Omega$ cm which is comparable to the minimum resistivity reported for the Sb_2O_3-doped $BaTiO_3$ [10]. The ionic radii of Ba^{2+}, Sb^{3+}, Ti^{4+}, and Mg^{2+} ions are 0.135, 0.076, 0.065, and 0.069 nm, respectively [13]. The trivalent Sb^{3+} ions tend to occupy the position of Ba^{2+} in preference to Ti^{4+} ions, while Mg^{2+} would replace Ti^{4+} instead Ba^{2+}, as expected from the radii. Possible defect reactions are as follows [12]:

$$2Sb_2O_3 + 4TiO_2 \rightarrow 4Sb_{Ba}^{\cdot} + 4Ti_{Ti}^{X} + 12O_O^{X} + O_2 + 4e' \quad (1)$$

$$2MgO + 2BaO + O_2 \rightarrow 2Mg_{Ti}'' + 2Ba_{Ba}^{X} + 6O_O^{X} + 2h^{\cdot} \quad (2)$$

Magnesium ions behave as electron acceptors in $BaTiO_3$ and compensate some of the donor Sb^{3+} ions. Consequently, the antimony content for minimum resistivity of Sb_2O_3-MgO codoped $BaTiO_3$ is higher than that for Sb_2O_3-doped $BaTiO_3$.

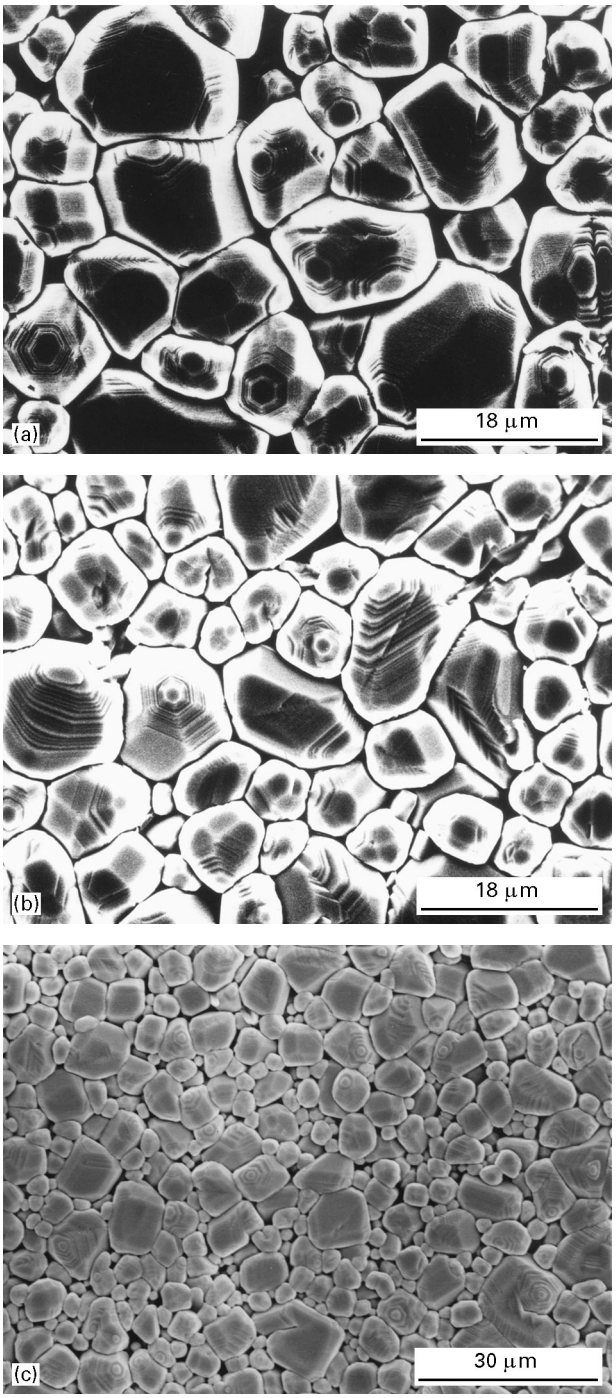

Figure 1 SEM micrographs for $BaTiO_3$ doped with 1.0 mole % MgO, 0.05 mole % MnO_2 and x mole % Sb_2O_3. (a) $x = 0.8$, (b) $x = 0.9$, and (c) $x = 1.0$.

The values of $\rho_{r.t}$, ρ_{max}, $\rho_{max}/\rho_{r.t}$, and T_{max} are summarized in Table II. The 0.9 mole % Sb_2O_3 sample has the smallest resistivity increase $\rho_{max}/\rho_{r.t}$ and the largest T_{max} among the compositions studied. Also, a strong NTCR effect is noticeable for the specimen with 1.0 mole % Sb_2O_3 after the maximum resistivity is reached at about 200 °C, as shown in Fig. 5.

The PTCR effect has been confirmed to originate from the grain boundary property and to be associated with the ferroelectric-pararelectric phase transition in semiconducting barium titanate ceramics [8, 14]. According to Heywang's [10, 11] model, the presence of grain boundary depletion layers consisting

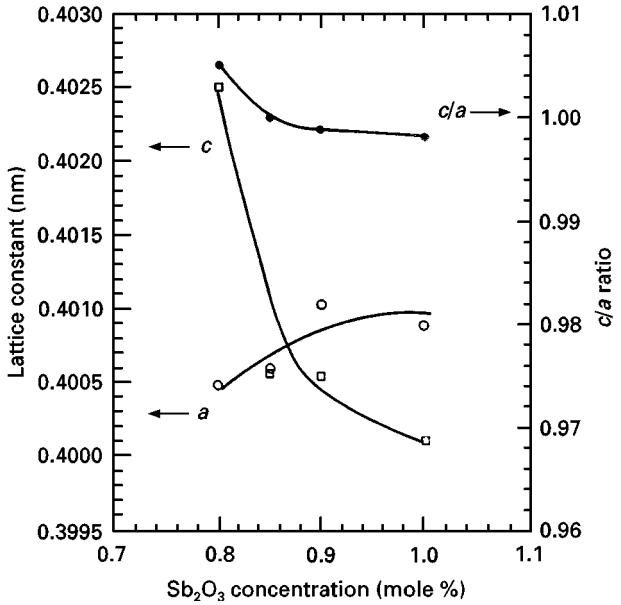

Figure 2 Lattice constant as a function of Sb_2O_3 concentration.

TABLE I Average grain size and density for $BaTiO_3$ doped with 1.0 mole % MgO, 0.05 mole % MnO_2 and various amounts of Sb_2O_3

Sb_2O_3 (mol %)	Average grain size (μm)	Theoretical density ($g\,cm^{-3}$)	Measured density ($g\,cm^{-3}$)	D_{th} (%)
0.8	9.2	5.99	5.66	94.5
0.9	7.0	6.00	5.75	95.8
1.0	5.0	6.01	5.86	97.5

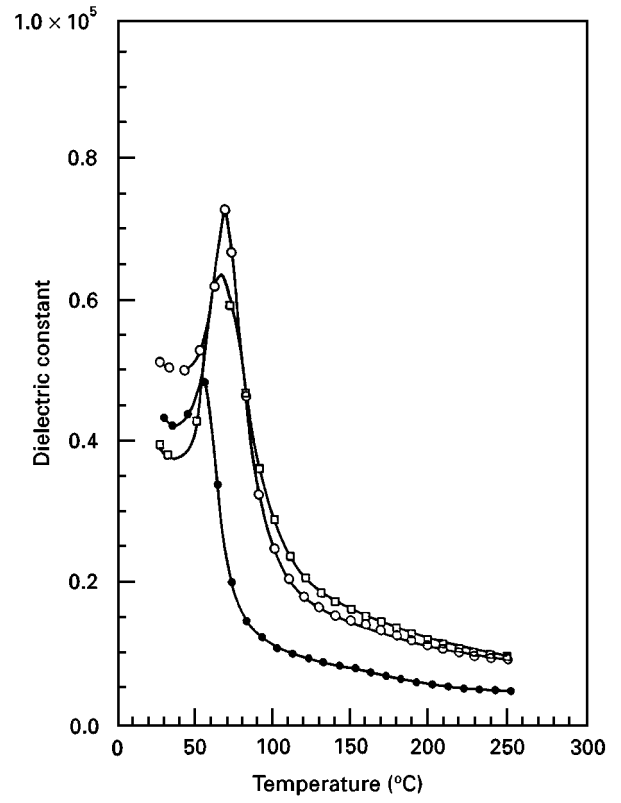

Figure 3 Apparent dielectric constant as a function of temperature for $BaTiO_3$ doped with 1.0 mole % MgO, 0.05 mole % MnO_2, and x mole % Sb_2O_3, where $x = 0.85$ (○), 0.9 (□) and 1.0 (●).

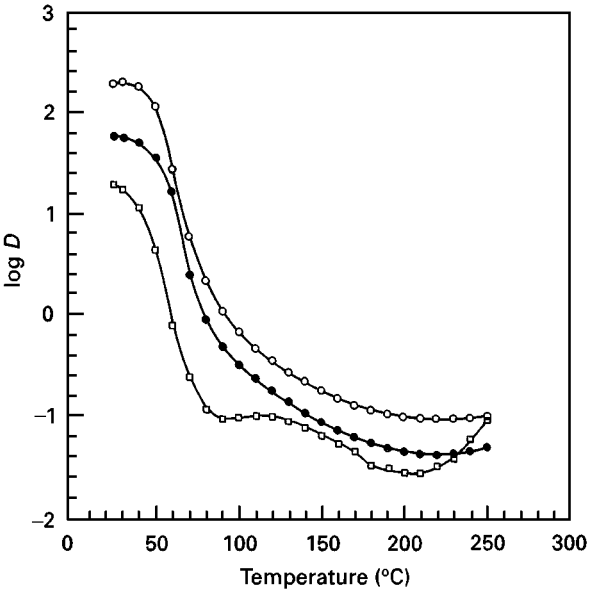

Figure 4 Dissipation factor as a function of temperature for $BaTiO_3$ doped with 0.1 mole % MgO, 0.05 mole % MnO_2 and x mole % Sb_2O_3 at 1 kHz: (●) $x = 0.85$, (○) $x = 0.9$. and (□) $x = 1.0$.

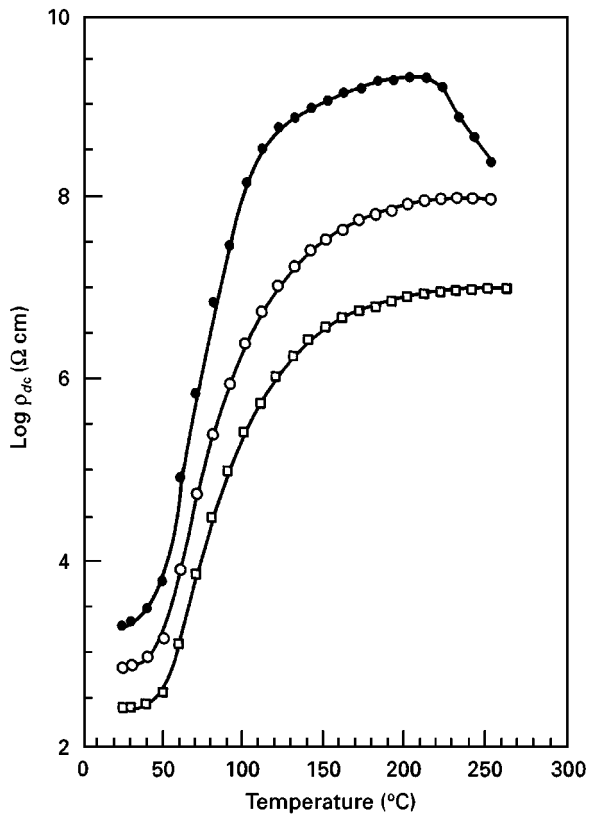

Figure 5 Resistivity as a function of temperature for $BaTiO_3$ doped with 1.0 mole % MgO, 0.05 mole % MnO_2 and x mole % Sb_2O_3: (○) $x = 0.85$, (□) $x = 0.9$, and (●) $x = 1.0$.

of two-dimensional surface acceptor states gives rise to a potential barrier at the grain boundary as a result of the upward bending of the conduction band, as shown schematically in Fig. 6 [15].

The charge in the surface states equals the charge in the depletion region. Below T_c, the potential barrier is compensated by the charges arising from the

TABLE II Logarithm of room temperature resistivity $\rho_{r.t}$, maximum resistivity ρ_{max}, resistivity increase $\rho_{max}/\rho_{r.t}$ and temperature of maximum resistivity T_{max} for $BaTiO_3$ doped with 1.0 mole % MgO, 0.05 mole % MnO_2 and various amounts of Sb_2O_3

Sb_2O_3 (mol %)	log $\rho_{r.t}$ (Ω cm)	log ρ_{max} (Ω cm)	log $\rho_{max}/\rho_{r.t}$	T_{max} (°C)
0.85	2.8	8.0	5.2	230
0.9	2.4	7.0	4.6	250
1.0	3.3	9.2	5.9	200

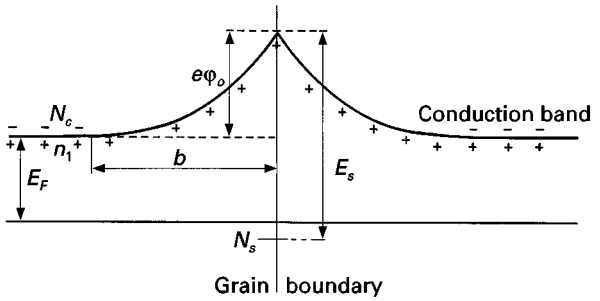

Figure 6 Energy level diagram near a grain boundary [15].

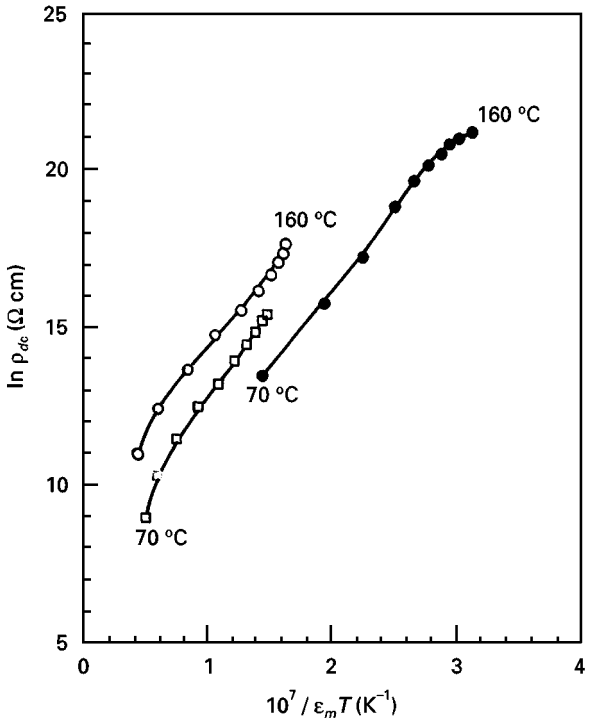

Figure 7 Plots of $\ln(\rho_{dc})$ against $1/\varepsilon_m T$ for $BaTiO_3$ doped with 1.0 mole % MgO, 0.05 mole % MnO_2, and x mole % Sb_2O_3: (○) $x = 0.85$, (□) $x = 0.9$, and (●)$x = 1.0$. Dielectric constant ε_m is measured at 1 kHz.

spontaneous polarization, rendering the whole material conductive. Above T_c, the spontaneous polarization disappears and the resistivity is controlled by the potential barrier. The barrier height Φ_o is [6, 7, 16]

$$\Phi_o = en^2/8\varepsilon_o n\varepsilon_r \tag{3}$$

and the barrier thickness b is

$$b = n_s/2n \tag{4}$$

where e is the electron charge, n (cm^{-3}) the effective donor concentration within the grain, ε_o the permittivity of free space, n_s number of electrons trapped in the surface states (number is N_s at a distance E_s below the conduction level), ε_r the relative permittivity, and

$$\varepsilon_r = C/T - T_c \tag{5}$$

where C is the Curie constant and T is the absolute temperature. The measured dielectric constant ε_m of a material consisting of insulating grain-boundary layers and a semiconducting grain is [18]

$$\varepsilon_m = \varepsilon_{gb} d/t \tag{6}$$

where d is the average grain size of the dielectric and ε_{gb} and t are the dielectric constant and thickness of the insulating grain boundary layer, respectively. In this case,

$$t = 2b \tag{7}$$

$$\varepsilon_{gb} = \varepsilon_r \tag{8}$$

and

$$\varepsilon_m = \varepsilon_r\,(d/2b) \tag{9}$$

The dielectric constants of samples in this study are one to two orders of magnitude larger than those of the undoped $BaTiO_3$ at T_c (i.e. 1000 ~ 5000) [11]. Yamamoto and Takao [19] estimated a grain boundary layer of ~0.26 μm thickness for a PTC thermistor. The average grain size of the 0.9 mole % Sb_2O_3-doped sample is 7.0 μm. Substituting these data into Equation 9 one obtains ε_m values of around 1.3×10^4 to 6.7×10^4 which are in agreement with the measured data shown Fig. 3. This suggests that the $BaTiO_3$ ceramic exhibits the characteristics of the so-called grain boundary barrier layer (GBBL) capacitors [18]. From semiconductor theory, the resistivity of the depletion layer ρ_L is given by

$$\rho_L = \rho_o \exp(e\phi_o/kT) \tag{10}$$

For a polycrystalline sample with semiconducting grain and insulating barrier layers, the resistivity can be expressed as

$$\rho = \rho_g + \rho_L \approx \rho_L \tag{11}$$

where ρ_g is the resistivity of the grain.

Combining Equations 4, 9, 10 and 11 into Equation 3, one has

$$\rho = \rho_o \exp(e\phi_o/kT) = \rho_o \exp(An_s/\varepsilon_m T) \tag{12}$$

$$A = e^2 d/8k\varepsilon_0 \tag{13}$$

Fig. 7 is the $\ln(\rho_{dc})$ versus $1/\varepsilon_m T$ plots. It is seen that the slopes of the curves decrease as temperature increases from T_c to T_{max}. This suggests a decrease of the grain boundary acceptor states n_s with temperature.

Previous work reported a value of n_s to be about $10^{14}\,cm^{-2}$ and n of $\sim 3 \times 10^{19}\,cm^{-3}$ for $BaTiO_3$ doped with 0.07 wt % Sb_2O_3 [19]. In this study, the n_s at T_c is $\sim 4 \times 10^{13}\,cm^{-2}$ which is of the same order as literature reported data [19]. However, the effective donor concentration n, estimated on the basis of

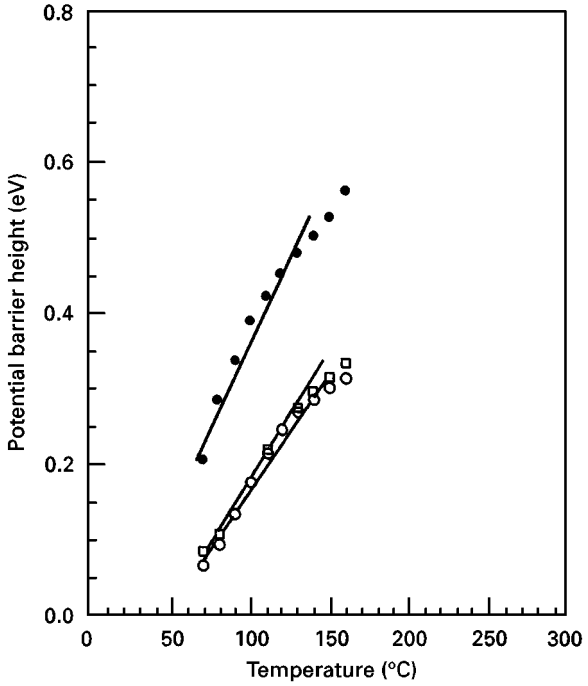

Figure 8 The potential barrier height as a function of temperature for $BaTiO_3$ doped with 1.0 mole % MgO, 0.05 mole % MnO_2, and x mole % Sb_2O_3: (○) $x = 0.85$, (□) $x = 0.9$, and (●)$x = 1.0$.

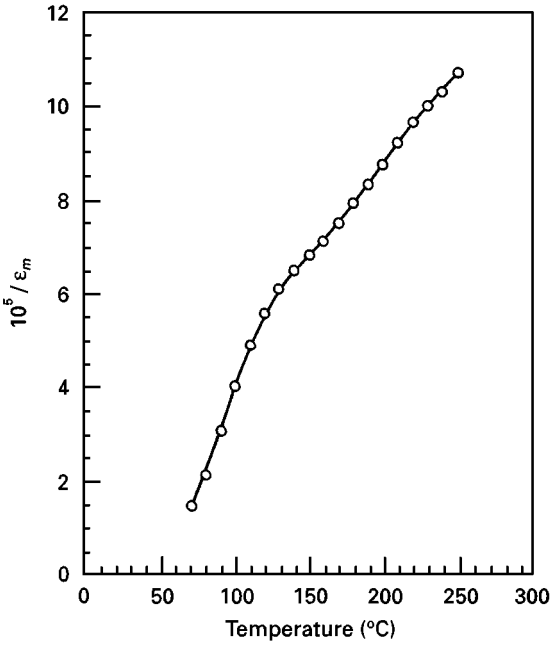

Figure 9 Reciprocal of the dielectric constant as a function of temperature for $BaTiO_3$ doped with 1.0 mole % MgO, 0.05 mole % MnO_2, and 0.85 mole % Sb_2O_3.

dielectric data in Fig. 4 and Equations 4 and 9, is $\sim 2 \times 10^{17}$ cm^{-3} which is much smaller than reported data [19]. This confirms that not all of the Sb_2O_3 addition was effective in making the ceramics semiconducting. Only part of the Sb_2O_3 addition was effective as donors. Magnesium ions behave as electron acceptors in $BaTiO_3$ ceramics, and compensate some of the donor Sb^{3+} ions.

The barrier height Φ_o is calculated on the basis of Equation 3 and plotted as a function of temperature, as shown in Fig. 8. Combining Equations 3 and 5, one has

$$\Phi_o = en_s\,(T - T_c)/8Cn\varepsilon_o \qquad (14)$$

which indicates that, for given values of n and n_s, Φ_o is directly proportional to temperature. However, since n_s decreases as temperature increases, the increase of Φ_o with temperature is not as great at elevated temperatures. Hence, a slower increase in Φ_o is observed at temperatures higher than 140 °C, as shown in Fig. 8. In addition, the barrier height increases as the Sb_2O_3 concentration is raised from 0.9 mole % to 1.0 mole %.

The relation between $1/\varepsilon_m$ and temperature at $T > T_c$, exhibited in Fig. 9, indicates that the Curie–Weiss law is obeyed at temperatures in the range between 70 °C and 130 °C. At higher temperatures, $1/\varepsilon_m$ still increases linearly, but more slowly with temperature, giving a second region with smaller slope. The number of surface states n_s can be expressed as [15]:

$$n_s = N_s/\{1 + \exp[(E_f + e\Phi - E_s)/kT\,]\} \qquad (15)$$

Equation 9 can be rewritten as:

$$\varepsilon_m = \varepsilon_r(dn/n_s) \qquad (16)$$

At lower temperatures, the acceptor states at the grain surface are almost fully ionized, i.e. $n_s \approx N_s$, and ε_m is expected to follow the Curie–Weiss law. However, at sufficiently high temperatures, $E_f + e\Phi$ approaches E_s and depopulation of surface states occurs (Fig. 6). The decrease in n_s with rising temperature counteracts the reduction of ε_m. Hence, $1/\varepsilon_m$ rises more slowly with temperature once depopulation of the surface states begins.

4. Conclusions

1. $BaTiO_3$ doped with 1.0 mole % MgO, 0.05 mole % MnO_2, and various amounts of Sb_2O_3 were fabricated with a two-stage firing profile. The Curie temperature and grain size decrease with the increase of Sb_2O_3 content.
2. For the Sb_2O_3–MgO codoped samples, the minimum resistivity, smallest resistivity increase $\rho_{max}/\rho_{r.t}$ and the largest T_{max} occur at 0.9 mole % Sb_2O_3 for 1 mole % MgO addition.
3. Magnesium ions, substituting as the Ti^{4+} sites, behave as electron acceptors in $BaTiO_3$ and compensate some of the donor Sb^{3+} ions. This results in smaller donor concentrations than in other reported work.
4. The measured dielectric constant ε_m is inversely proportional to temperature as predicted by the Curie–Weiss law. However, as depopulation of surface states occurs, $1/\varepsilon_m$ rises more slowly with temperature at higher T.

Acknowledgment

This work is supported by the National Science Council, Taiwan, under the contract NO. NSC 85-2216-E-009-012.

References

1. B. M. KULWICKI, in "Grain Boundary Phenomena in Electronic Ceramics", Adv. in Ceramics, Vol. 1, edited by L. Levinson (American Ceramic Society, Inc., Columbus, OH. 1981) pp. 135–154.
2. D. C. HILL and H. L. TULLER, in "Ceramic Sensors: Theory and Practice", Ceramic Materials for Electronics-Processing, Properties, and Applications, edited by R. C. Buchnan (Marcell Dekker, Inc., New York, 1986) pp. 265–374.
3. M. KUWABARA, *J. Am. Ceram. Soc.* **71** (1988) C110.
4. H. M. AL-ALLAK, T. V. PARRY, G. J. RUSSEL and J. WOODS, *J. Mater. Sci.* **23** (1988) 1083.
5. T. MATSUOKA, Y. MATSUO, H. SASAKI and HAYAKAWA, *J. Am. Ceam. Soc.* **55** (1972) 108.
6. H. F. CHENG, *J. Appl. Phys.* **66** (1989) 1382.
7. B. S. CHIOU, C. M. KOH and J. G. DUH, *J. Mater. Sci.* **22** (1987) 3893.
8. C. J. KIM and K. NO, *ibid* **28** (1993) 5765.
9. A. B. ALLES, V. R. W. AMARAKOON and V. L. BURDICK, *J. Am. Ceram. Soc.* **72** (1989) 148.
10. W. HEYWANG, *ibid.* **47** (1964) 484.
11. W. HEYWANG, *J. Mater. Sci.* **6** (1971) 1214.
12. C. J. TING, C. J. PENG, H. Y. LU and S. T. WU, *J. Am. Ceram. Soc.* **73** (1990) 329.
13. W. D. KINGERY, H. K. BOWEN and D. R. UHLMANN, "Introduction to Ceramics", 2nd Edn (John Wiley & Sons, Inc., New York, 1976) p. 58.
14. A. B. ALLES and V. L. BURDICK, *J. Am. Ceram. Soc.* **76** (1993) 401.
15. G. H. JONKER, *Solid State Electron.* **7** (1964) 895.
16. G. H. LEWIS and C. R. A. CATLOW, *J. Am. Ceram. Soc.* **68** (1985) 555.
17. J. ILLINGSWORTH, H. M. AL-ALLAK, A. W. BRINKMAN and J. WOODS, *J. Appl. Phys.* **67** (1990) 2088.
18. B. S. CHIOU, S. T. LIN, J. G. DUH and P. H. CHANG, *J. Am. Ceram. Soc.* **72** (1989) 1967.
19. T. YAMAMOTO and S. TAKAO, *Jpn. J. Appl. Phys.* **31** (1992) 3120.

Received 18 April
and accepted 23 July 1997